Visual Neuroscience (1993), **10**, 653-667. Printed in the USA.

Phototransduction and adaptation in rods, single cones, and twin cones of the striped bass retina: A comparative study

JAMES L. MILLER AND JUAN I. KORENBROT

Department of Physiology, School of Medicine, University of California at San Francisco, San Francisco

(RECEIVED September 16, 1992; ACCEPTED November 19, 1992)

Abstract

We investigated the attributes of transduction and light-adaptation in rods, single cones, and twin cones isolated from the retina of striped bass (*Morone saxatilis*). Outer-segment membrane currents were measured with suction electrodes under voltage clamp provided by tight-seal electrodes applied to the cell's inner segment. Brief flashes of light transiently reduced the outer-segment current with kinetics and sensitivity characteristic of each receptor type. In all cells, the responses to dim lights increased linearly with light intensity. The amplitude-intensity relation for rods and single cones were well described by an exponential saturation function, while for twin cones it was best described by a Michaelis-Menten function. At the wavelength of maximum absorbance, the average intensity necessary to half-saturate the peak photocurrent in dark-adapted rods was 28 photons/μm^2 and in single cones it was 238 photons/μm^2. Among twin cones, the common type (88% of all twins recorded) half-saturated at an average of 1454 photons/μm^2, while the fast type reached half-saturation at an average of 9402 photons/μm^2. The action spectrum of the photocurrent in the three receptor types was well fit by a nomogram that describes the absorption spectrum of a vitamin A_2-based photopigment. The wavelength of maximum absorbance for rods was 528 nm, for single cones it was 542 nm and for twin cones it was 605 nm. Both members of the twin pair contained the same photopigment and they were electrically coupled. Under voltage clamp, the response to dim flashes of light in both single and twin cones was biphasic. The initial peak was followed by a smaller amplitude undershoot. Single cones reached peak in 86 ms and common twins in 50 ms. Background light desensitized the flash sensitivity in all photoreceptor types, but was most effective in rods and least effective in fast twins. In the steady state, the desensitizing effect of a background intensity, *Ib*, at the respective optimum wavelength for each cell was well described by the Weber-Fechner law ($1/(1 + Ib/Ibo)$), where *Ibo* was, on average (in units of photons/μm^2/s), 1.45 for rods, 1.81×10^3 for single cones, 4.56×10^3 for common twins, and 6.79×10^4 for fast twins.

Keywords: Retina, Phototransduction, Teleost, Photoreceptors, Light adaptation

Introduction

In the vertebrate retina there exist two functionally and anatomically distinct types of photoreceptor cells, rods and cones (Walls, 1942; Cohen, 1972; Rodieck, 1973). In a given species, photoresponses of each receptor type are profoundly different; in general, the response of the rods is slower, more sensitive to light, and adapts over a more restricted range of light intensities than that of the cones. Interestingly, the attributes of the rod's response to light such as action spectrum, absolute light sensitivity, and time course are remarkably constant when compared across species (reviews in Baylor, 1987; McNaughton, 1990). The attributes of the cone photoresponse, in contrast, vary widely across species. Indeed, cones of functional subtypes can coexist in the same retina. For example, retinae of cold-blooded vertebrates may contain cone pairs consisting of either anatomically identical members (twin cones) or nonidentical members (double cones), in addition to several types of single cones, each tuned to particular wavelengths of light (Walls, 1942; Ali & Anctil, 1976). In some species, each member of a cone pair contains the same photopigment, while in others different photopigments are found in each member (Levine et al., 1979; Loew & Lythgoe, 1978; Burkhardt et al., 1980).

Despite great progress towards elucidating the mechanisms of transduction in rod photoreceptors (reviews in Pugh & Cobbs, 1986; Pugh & Lamb, 1990; McNaughton, 1990), an explanation for the difference in transduction signals between rods and cones and between cone subtypes in a given species is not at hand

Reprint requests to: Juan I. Korenbrot, Dept. of Physiology, School of Medicine, Box 0444, University of California at San Francisco, San Francisco, CA 94143, USA.

(Hestrin & Korenbrot, 1990). This is due, in part, to technical limitations: in only one species, the tiger salamander, have both rods and cones been studied electrophysiologically under voltage clamp (Baylor & Nunn, 1986; Attwell et al., 1982), a condition necessary to reveal the true time course and photosensitivity of the change in membrane current caused by light. However, tiger salamander cones are relatively small and, therefore, many of the experimental manipulations necessary to study transduction in single cells are not possible in this species. Another limitation arises from the fact that there does not exist a preparation of isolated, purified cones readily accessible to biochemical investigation. As part of our effort to develop a preparation to further our understanding of transduction in cones, we report here on the features of the transduction signals in the photoreceptors of the striped bass (*Morone saxatilis*). This retina contains rods and two types of cones: single and twin. The photoreceptors can be isolated in large numbers and maintained physiologically viable for many hours in culture. Individual cones, both single and twins, are very large and stable electrical recordings can be easily accomplished. In parallel work, we have employed this preparation to study the control of cone outer-segment cGMP concentration by calcium (Miller & Korenbrot, 1992) and the monovalent cation selectivity of the cGMP-regulated conductance (Picones & Korenbrot, 1992). Also, we have developed a preparation of isolated cones in sufficient quantity and purity to support biochemical studies of phototransduction (in preparation).

Phototransduction in single and twin cones of fish has been studied in the past only with intracellular measurements of membrane voltage. Indeed, the very first successful recordings from photoreceptor cells were obtained from cones in the eyecup of carp (*Cyprinus carpio;* Tomita, 1970). In addition to recent recordings from the carp retina (Kaneko & Tachibana, 1985), intracellular recordings have also been obtained from the single and twin cones of the walleye (*Stizostedion vitreum vitreum*, Burkhardt et al., 1980; Burkhardt et al., 1986), and the single and double cones of the tench (*Tinca tinca*, Marchiafava et al., 1985). We report here the first investigation of the transduction currents of isolated fish cone photoreceptors measured under voltage clamp. We show that the transduction signals in rods and in each of the cone subtypes differ significantly with respect to light sensitivity, photopigment absorbance properties, response kinetics, and light adaptation. We also provide evidence that the members of twin pairs are electrically coupled.

Methods

Materials

Striped bass (*Morone saxitilis*, 5–18 months old, 5–25 cm body length), obtained from a fish hatchery (Professional Aquaculture Services, Chico, CA), were held under 12-h light/12-h dark cycles at 20°C and fed *ad lib*. DNAse I (Type IV) and hyaluronidase (Type 1-S, 290 Units/mg) were obtained from Sigma (St. Louis, MO). Collagenase (CLSS, 130 Units/mg) was purchased from Worthington Biochemicals (Freehold, NJ) and wheat germ agglutinin (WGA) from E.Y. Labs. (San Mateo, CA). MEM vitamins and amino-acid supplements were obtained from the Tissue Culture Facility at University of California at San Francisco.

Solutions

The ionic composition of our standard bathing solution (fish Ringer's) was 136 mM NaCl, 2.4 mM KCl, 5 mM $NaHCO_3$, 1 mM NaH_2PO_4, 1 mM $MgCl_2$, 1 mM $CaCl_2$, 10 mM glucose, and 10 mM HEPES supplemented with bovine serum albumin (0.1 mg/ml) and Minimum Essential Medium vitamins and amino acids. The solution was titrated to pH 7.5 and its osmotic pressure was 309 mOsM. Tight-seal electrodes were filled with a solution containing 105 mM K-gluconate, 20 mM K-aspartate, 10 mM KCl, 10 mM NaCl, 4 mM $MgCl_2$, 3 mM Na_2-ATP, 1 mM Na_3-GTP, 10 mM MOPS, and 303 mOsM osmotic pressure. Solutions of pH 6.75 or 7.25 were used with identical results.

Dissociation of retinal photoreceptor cells and cell plating

Animals were dark-adapted for 90–120 min in an aerated, light-proof aquarium. In darkness, they were then anesthetized by immersion in ice water and sacrificed by decapitation and pithing. Dissections were performed under infrared illumination with the aid of an infrared-sensitive TV camera and video monitor. The retina was isolated by cutting the eyecup into quarters under fish Ringer's solution and collecting the dorsal-temporal quadrant which generally floated free from the eyecup. The retina section was processed using either of two protocols. (1) For experiments with suction electrodes alone, the retina was incubated in about 7 ml of fish Ringer's solution supplemented with 0.4 mg/ml each of collagenase, hyaluronidase, and DNAse I for 90 s and was then gently shredded with fine forceps in the same solution. The resulting small retinal fragments and dissociated cells were transferred directly to the recording chamber. (2) For experiments with simultaneous use of suction and tight-seal electrodes, the retina section was incubated in the enzyme containing solution described above and, after 90 s, it was transferred through three successive, 10-ml volumes of fish Ringer's solution free of enzyme and in which glucose was iso-osmotically replaced by sodium pyruvate (5 mM). The retina was finally transferred to 700 μl of the glucose-free Ringer's solution and shredded with fine forceps. 250 μl of the resulting suspension of dissociated photoreceptors were transferred onto a coverslip coated with 1 mg/ml WGA according to the method of Cherr and Cross (1987). The coverslip constituted the floor of a recording chamber. Dissociated photoreceptor cells were allowed to settle onto the coverslip for 15–20 min. Following the plating period, the pyruvate Ringer's solution was gently exchanged for the standard, glucose-containing fish Ringer's solution.

Electrical recordings

For experiments with suction electrodes alone, the recording chamber was similar to that described by Miller and Korenbrot (1987). For experiments with simultaneous use of suction and tight-seal electrodes, the recording chamber was held on the stage of an inverted microscope equipped with DIC optics. Cells were observed under infrared illumination (860–920 nm) with the aid of a TV camera and monitor. The chamber volume was about 0.5 ml and it was intermittently perfused with the standard incubating solution at a rate of 1–2 ml/min. Membrane currents were recorded from solitary single cones simultaneously

with extracellular suction electrodes (Baylor et al., 1979) and tight-seal electrodes in the whole-cell configuration (Hamill et al., 1981).

Extracellular membrane currents were measured with suction electrodes (Baylor et al., 1979) with typical tip openings forged to 4.5–6 μm for single cones and 6–8 μm for twin cones. Suction electrodes were filled with the fish Ringer's solution and placed within a holder that was connected, through a side arm, to micrometer syringes (Gilmont Instruments, Great Neck, NY) used to control the pressure within the electrode. An Ag/AgCl pellet was separated from the fluid within the suction electrode by a short (5 mm) Ringer's agar (2%) bridge. Rods were studied in clusters consisting of 3–6 individual cells in a small retinal piece. With single cones the electrode formed a 3–5 $\times$ 10^6 Ω seal against the distal region of the inner segment. With twin cones, the outer segments of both members of the pair were drawn into the electrode, which formed a 5–10 $\times$ 10^6 Ω seal against the distal portion of the inner segments. Tight-seal electrodes (Hamill et al., 1981) were fabricated from Corning 1724 glass (aluminosilicate, 1.5/1.0 mm o.d./i.d.) with typical tip openings of 0.8–1 μm (tip resistance 3–5 MΩ). For simultaneous recordings with suction and tight-seal electrodes, single or twin cones were first drawn into the suction electrode. Photocurrents were measured, and if the cells were determined to be healthy, a giga-seal was then formed with the tight-seal electrode placed against the base of the inner segment. Whole-cell recordings were established with a brief (0.1 ms) voltage pulse.

Membrane currents in the suction electrode were measured with a current amplifier (Dagan Model 8900, Dagan Corp., Minneapolis, MN) and further amplified by a high-impedance, low-noise amplifier (Model 113, EG&G, Princeton, NJ). The tight-seal electrode was connected to a patch-clamp amplifier (Axopatch 1-D, Axon Instruments, Foster City, CA). Analog signals were filtered using an 8-pole Bessel filter (Model LPF 902, Frequency Devices, Haverhill, MA, or Model 3341, Krohn-Hite, Avon, MA) at 50 to 100 Hz for suction electrode measurements or 300 Hz for the tight-seal electrode. Data were digitized on-line at 625 Hz with 12-bit accuracy and stored for later analysis (Fastlab System, Indec, Inc., Mountain View, CA). We used computer-aided, least-square minimization algorithms to fit mathematical functions to experimental data (NFit, Island Products, Galveston, TX). By convention, the dark current measured with suction electrodes engulfing the outer segment was defined as zero and the photocurrent as positive in polarity. The whole-cell current measured with tight-seal electrodes at −40 mV holding voltage was nearly zero, photocurrents were outwardly directed and are displayed as positive in polarity. In reality, photocurrents arise from the cessation of a sustained inward dark current through the outer-segment membrane (Hagins et al., 1970).

Photostimulation

Photoreceptors were stimulated with unpolarized light uniformly delivered to the entire cell. Two independent optical rails were assembled that delivered light through a final common path. Stimulus duration was controlled with electronic shutters mounted in the optical rail. Test flashes and adapting light steps were spectrally isolated using narrowband interference filters (±10 nm half-bandwidth) and intensity was controlled by calibrated neutral density filters. Test and adapting light intensities at various wavelengths between 480 nm and 700 nm were measured daily with a calibrated photodiode (UDT UV 100, United Detector Technologies, Hawthorne, CA).

Photosensitivity: relationship between response amplitude and stimulus intensity

To conduct this analysis, we measured the peak amplitude of photocurrents generated by 10-ms flashes of varying intensity. We normalized response amplitude by dividing the peak amplitude at each intensity by the saturating response measured in the cell. The relationship between normalized photocurrent peak amplitude and light intensity has been previously described by either of two empirical functions. The first is the exponential saturation function (Lamb et al., 1981):

$$\frac{i}{i_{max}} = 1 - \exp(-I * P), \tag{1}$$

where i/i_{max} is the normalized photocurrent amplitude, I is the flash intensity, in units of photons/μm^2, and $1/P$ is a constant that characterizes the flash photosensitivity of the cell, and corresponds to that intensity which elicits a response that is $0.632 i_{max}$ in amplitude.

The second is the Michaelis-Menten function (Baylor & Fuortes, 1970):

$$\frac{i}{i_{max}} = \frac{I}{I + \sigma}, \tag{2}$$

where i/i_{max} is the normalized photocurrent, I is the photon density of the flash, in units of photons/μm^2, and σ is the photon density necessary to produce a response amplitude that is half of the saturated amplitude. σ in eqn. (2) is related to P in eqn. (1) by

$$\sigma = \frac{\ln 2}{P}. \tag{3}$$

Both photosensitivity functions indicate that the amplitude of the photoresponse increases linearly with light intensity at dim light levels. Photocurrents generated by flashes within this intensity range are referred to as linear range responses.

Action spectra

To construct action spectra we used two different protocols. In the first one, amplitude-intensity curves were measured with 10-ms flashes of light at various wavelengths, and the experimental data fit with eqn. (1) for rods and single cones, or eqn. (2) for twin cones. From the fitted functions, we determined the flash intensity necessary to generate a criterion response and plotted this intensity at each wavelength by the smallest intensity measured. In the second, less elaborate method, we elicited linear range response and directly measured the flash sensitivity (pA/photons^{-1}/μm^2) of the cell at each wavelength tested. For each cell, we normalized the data by dividing the flash sensitivity at each wavelength by the highest sensitivity measured. Action spectra were fit with a polynomial expression of the Dartnall nomogram (Dawis, 1981).

Photocurrent kinetics

The time course of linear-range photocurrents measured in the absence of voltage clamp were fit by a function that describes the impulse response of a Poisson filter with "n" stages as first described by Baylor et al. (1974). This function has been found satisfactory in the description of the response waveform in vertebrate photoreceptors (Baylor et al., 1979, 1984):

$$i(t) = I * S_f^D * \left[\frac{t}{t_{peak}} * \exp\left(1 - \frac{t}{t_{peak}}\right)\right]^{n-1}, \quad (4)$$

where $i(t)$ is the time-dependent photocurrent (in pA), I is the intensity of the light flash (in units of photons/μm^2), S_f^D is the flash sensitivity of the dark-adapted cell (in units of pA/(photon/μm^2)), t_{peak} is the time-to-peak of the photocurrent, and n is the number of reactions. In fitting data, the product of $I * S_f^D$ is represented by a single amplitude term, A (in pA).

We developed an empirical description of the time course of voltage-clamped photocurrents as the sum of two impulse-response functions in which the amplitude of the second impulse response, corresponding to the oscillatory undershoot of baseline was time dependent and increased with a first-order time constant:

$$i(t) = A_1\left[\frac{t}{t_{peak1}} * \exp\left(1 - \frac{t}{t_{peak1}}\right)\right]^{n_1-1} + A_2\left(1 - \exp\frac{t}{\tau}\right)\left[\frac{t}{t_{peak2}} * \exp\left(1 - \frac{t}{t_{peak2}}\right)\right]^{n_2-1}, \quad (5)$$

where A_1 is the amplitude of the first impulse response, τ is the time constant of the second impulse response of amplitude A_2, and t_{peak1} and t_{peak2} correspond to the times of the response maximum and minimum, respectively.

Light adaptation

In these studies, a step of light 3.5 s in duration of controlled intensity and wavelength was presented to the photoreceptor. Two seconds after the onset of the adapting light, a time sufficient for the photocurrent to reach steady state, we delivered a 10-ms flash that elicited a linear-range response. The flash sensitivity of the cell was measured for each background step of light tested. The adapting steps of light were limited to intensities that allowed full recovery of the dark-adapted flash sensitivity when the adapting light was turned off. The changes in flash sensitivity as a function of the intensity of the adapting background were well described by the Weber-Fechner relation:

$$\frac{S_f}{S_f^D} = \frac{1}{\left[1 + \frac{I_b}{I_{bo}}\right]}, \quad (6)$$

where S_f^D is the flash sensitivity (pA·photon^{-1}·μm^2) of the dark-adapted cell, S_f is the flash sensitivity of the cell in the presence of a background light of intensity I_b (photons $\mu m^{-2}\cdot s^{-1}$), and I_{bo} is the intensity of adapting light that reduces the flash sensitivity by 50%.

Results

Light-microscopic evaluation of striped bass retinal photoreceptor cells

Mild, brief enzymatic digestion followed by mechanical disruption of striped bass retinae yielded three types of dissociated photoreceptor cells recognized by their distinct anatomy: rods, single cones, and twin cones (Fig. 1). The dissociated photoreceptors were anatomically incomplete: they consisted of the outer segment, and the ellipsoid and myoid regions of the inner segment, but they lacked the nuclear and synaptic sections of the cells. Rods were the smallest and most plentiful of the photoreceptor cells in this retina, *ca.* 60×10^7 cells per retina in a 25-cm animal with average outer-segment dimensions of 1.6×40 μm (diameter × length). Single- and twin-cone populations in the striped base retina were both on the order of 3×10^7 cells per retina (25-cm animal). The size of cones, particularly twin cones, but not rods, increased with fish body length. The *average* size of the single cone outer segment was about 5×15 μm (base diameter × length) and a tip diameter of *ca.* 3 μm, giving an outer-segment volume of *ca.* 190 μm^3. The outer segments of the individual members of a twin pair had *average* dimensions of *ca.* 6×20 μm (base diameter × length), and a tip diameter of *ca.* 4 μm giving an outer-segment volume of *ca.* 300 μm^3. While the cone outer-segment dimensions reported above represent those of a *typical* single or twin outer segment, it was not uncommon to find particularly large twin cones containing outer segments as large as 8×40 μm (base diameter × length) tapering to 6 μm at the tip.

Photocurrents elicited by flashes of light

Typical photocurrents generated at room temperature by brief flashes of light of varying intensity in rods, single cones, and twin cones and measured with suction electrodes alone are illustrated in Fig. 2. The photocurrents measured in the dissociated photoreceptors were indistinguishable from those measured in cells that were associated with small retinal fragments. Each photoreceptor type generates transduction signals that are unique in their kinetics, photosensitivity, and light- and dark-adaptation properties. We discuss these differences in detail below.

Light sensitivity

Rods

Rod photocurrents were measured by gently drawing into the suction electrode a cluster of 3–5 rod outer segments, protruding from a small retinal slice. Rod responses illustrated in Fig. 2 were elicited by 10-ms duration flashes of 520-nm light, a color near the maximum absorbance of the photopigment in the cell (see below). Consistent with the behavior of other rod photoreceptors of comparable size, dim flashes generated photocurrents that developed smoothly, reached a peak in *ca.* 400 ms, and then decayed with a time course slower than that of the rising phase. As flash intensity increased, the rate of rise of the signal became steeper and the peak amplitude increased and shifted slightly to earlier times. Current amplitude reached a saturating value, when all dark current was suppressed and further increments in flash intensity extended the time over which the photocurrent remained saturated.

To measure light sensitivity, we measured the peak amplitude of the photoresponse as a function of stimulus intensity. To compare data among different clusters, we normalized the data for each cell cluster by dividing the current amplitude at each intensity by the saturated amplitude. Fig. 3 illustrates the normalized peak amplitude–intensity relationship of rods. The data were best fit by the exponential saturation function, eqn. (1) (Lamb et al., 1981). Least-square fit of the function to experimental data from 11 clusters of rods was obtained with values of $P = 0.024 \pm 0.0043$ (mean ± S.D., range = 0.018–0.039, derived $\sigma = 28.1 \pm 7.07$ photons/μm^2) (Table 1).

Single cones

Single-cone photocurrents illustrated in Fig. 2 were generated by 10-ms flashes that delivered varying intensities of 540-nm light, a color near the maximum absorbance of the photopigment in the cone (see below). The photocurrents increased smoothly to reach a peak in *ca.* 170 ms and then decayed to the preflash baseline with significantly slower kinetics than the rising phase. In contrast to the response of rod photoreceptors, the larger membrane capacitance of cones (56.53 pF ± 15.42, mean ± S.D., $n = 28$) leads to distortions in the kinetics of photocurrents measured in the absence of voltage clamp. The time constant of the cell membrane (input resistance at resting potential = $5.83 \pm 1.08 \times 10^8$ Ω mean ± S.D., $n = 13$, 32.9-ms time constant, on average) limits the rising phase kinetics of the photocurrent producing a superposition of the photocurrents at early times. Typical photocurrent saturated amplitudes in single cones ranged from 10.7–45 pA (23.3 ± 8.2, $n = 45$). Fig. 3 illustrates the normalized peak amplitude-intensity relationship of single cones. Data were best described by the exponential saturating function (Lamb et al., 1981). Least-square fit of this function to experimental data for 42 cells was obtained with values of $P = 0.00291 \pm 0.00101$ (derived $\sigma = 238.0 \pm 128.1$ photons/μm^2, mean ± S.D., range = 34.5–568) (Table 1).

Twin cones

Twin cones exhibited either of two functionally distinct responses to light. Of all twin cones we recorded from, 88% (151/172) exhibited photocurrents such as those illustrated in Fig. 2 and identified as common twins. Shown are photocurrents elicited by 10-ms duration flashes of 620 nm, a color near the maximum absorbance of the visual pigment in the twin cones. Photocurrents of these common twins were faster in time course and about sixfold less sensitive than those of single cones. The remaining 12% of twin cones (21/172) responded to light flashes with faster kinetics and were even less sensitive to light. Photocurrents elicited by 10-ms flashes of 620-nm light in this distinct subclass of twin cones are also shown in Fig. 2 and identified as fast twins.

In common twins, saturated photocurrent amplitude ranged from 12.3–84.8 pA (33.98 ± 16.7 pA; mean ± S.D., $n = 57$). The photocurrent reached to a peak in 90–120 ms and this time appeared essentially invariant for intensities producing photocur-

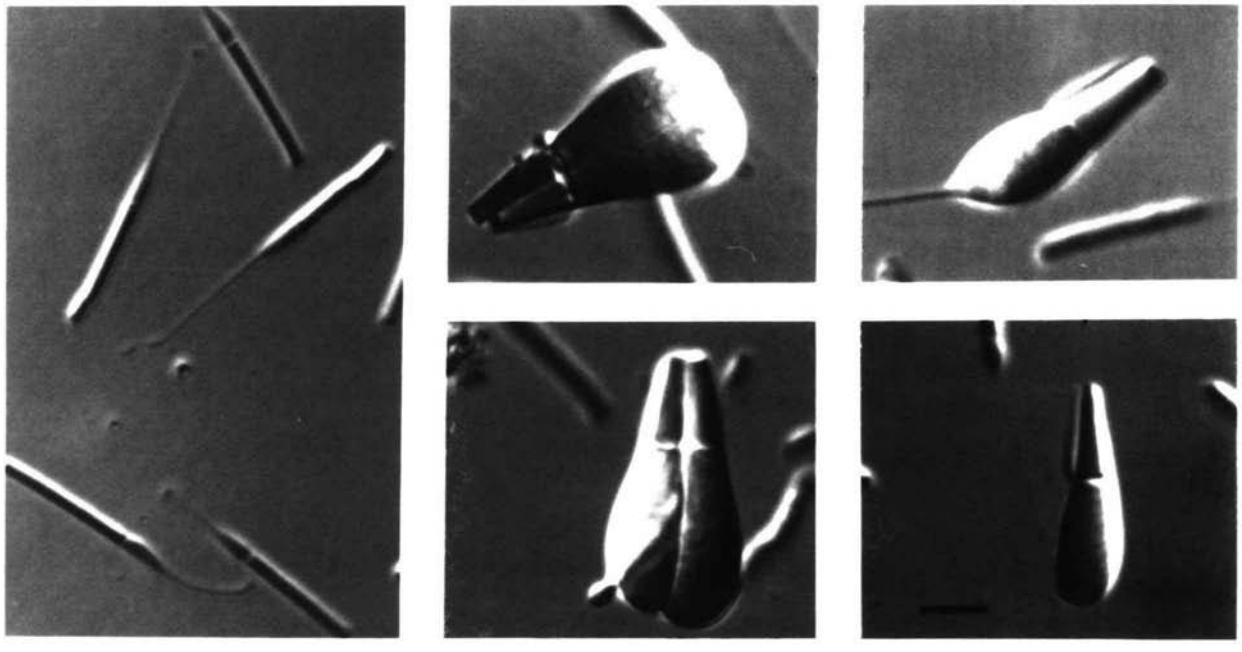

Fig. 1. Micrographs of isolated photoreceptors of the striped bass retina. Cells were dissociated from the retina of a 6-cm-long fish and micrographed with the aid of differential interference contrast enhancement. Shown in the left panel are rods, in the middle panel twin cones, and in the right panel single cones. The isolated rods consist of an outer segment and an incomplete inner segment with a stretched out myoid, the contractile element in the cell. The solitary cones consist of an outer segment and an incomplete inner segment, lacking the nucleus and synaptic pedicle. An accessory cone outer segment, appearing as a thin projection from the inner segment that runs parallel to the outer segment, can be recognized in both single and twin cones. In fish, the eye grows as body length increases (Lyall, 1957). As the eye grows, the size of single cones remains relatively constant, and the cells shown are typical of single cones found in all fish we studied (body lengths 5–25 cm). Twin cones, in contrast, increase in size as the eye grows (Lyall, 1957). The twin cones illustrated, therefore, are smaller than those found in larger fish; their appearance, however, is the same. Scale bar is 10 mm.

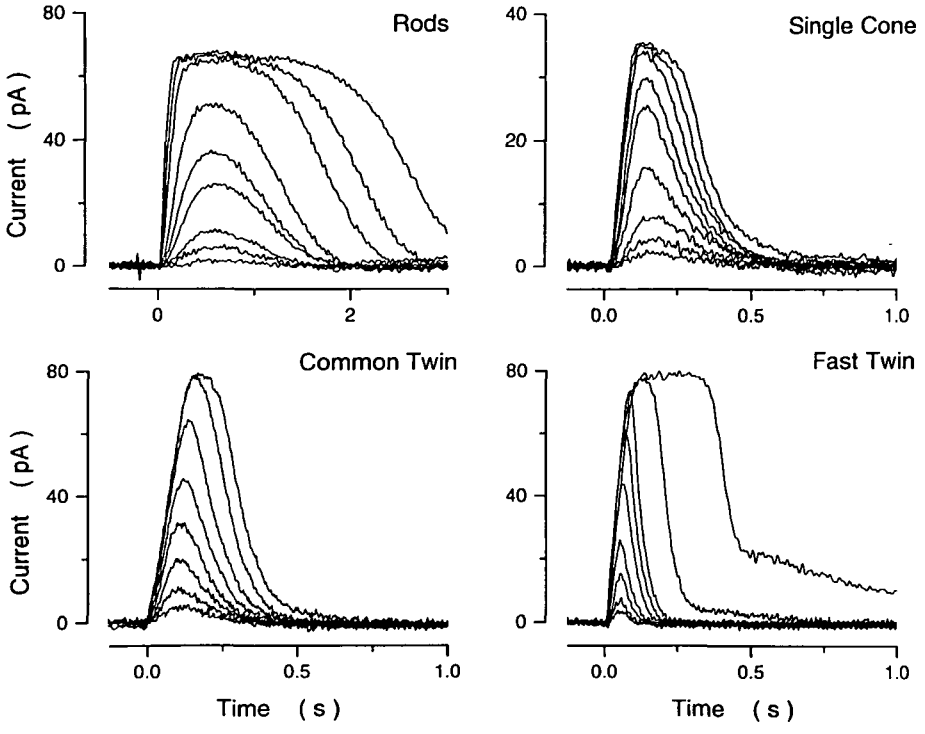

Fig. 2. Outer-segment photocurrents measured with suction electrodes in isolated photoreceptors of the striped bass. The rod photoresponses were measured by engulfing a cluster of three outer segments protruding from a retinal piece within the suction electrode. In rods, responses were elicited by 10-ms duration flashes of 523-nm light presented at time 0 that delivered 1.1, 2.2, 4.5, 9.8, 17.8, 35.6, 71, 143, and 285 photons/μm^2, respectively. The photocurrents in single cones were measured from one cell in response to 10-ms duration flashes of 540-nm light that delivered 32.3, 64.6, 129.1, 322.8, 646, 1291, 3228, 6455, and 12911 photons/μm^2. The photocurrents in twin cones, either the common or the fast type, were measured from a solitary cone pair with both outer segments within the suction electrode. In both types of twins responses were generated by 10-ms duration flashes of 620-nm light. The intensity of the flashes used for common twin were 152.3, 313.2, 622, 1302.6, 2623, 5198, 14921, and 30676 photons/μm^2, while for fast twins they were 952, 2379, 4759, 9518, 2.37 × 10^4, 4.75 × 10^4, 9.51 × 10^4, 1.3 × 10^6, and 5.4 × 10^6 photons/μm^2. All data were collected at room temperature (21°C).

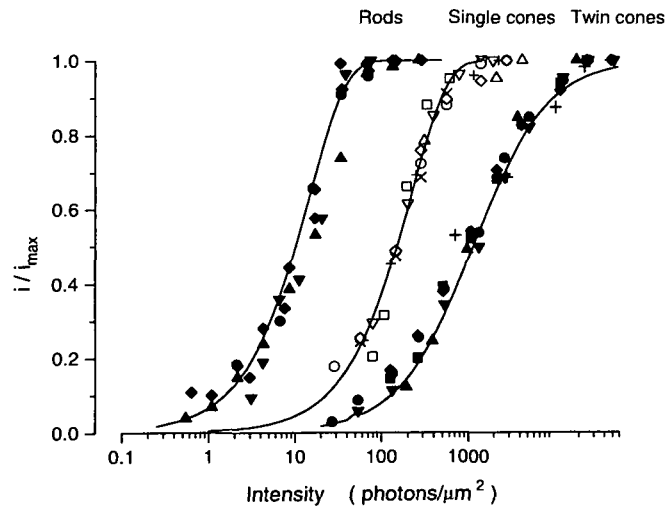

Fig. 3. Sensitivity of photocurrents in dark-adapted rods, single cones, and twin cones measured with suction electrodes. Photocurrent peak amplitude measured in each cell was normalized by the maximum peak amplitude measured in that cell. Light intensity was measured as the photon density (photons/μm^2) delivered in a 10-ms flash of a wavelength optimized for each photoreceptor type: 523 nm for rods, 537 nm for single cones, and 606 nm for twin cones. Each symbol identifies data from an individual cell. Continuous lines are least-square fits to the experimental data. Data from rods and single cones was best fit by the exponential saturation function [text eqn. (1)] with values of P = 0.0693 and P = 0.004, respectively. This value of P corresponds to an intensity necessary to half-saturate the peak amplitude of 10 photons/μm^2 for rods and 173 photons/μm^2 for single cones. Twin cone data were best fit by the Michaelis-Menten function [text eqn. (2)] with a value of σ, the intensity necessary to half-saturate the peak amplitude, of 1278 photons/μm^2.

rent amplitudes up to 50% of the saturated value. Photocurrents elicited by flashes of higher intensity exhibited pronounced increases in time to peak (Fig. 2). The time to peak in the photocurrent, however, is not a property of the transduction signal in these cells, but is a consequence of the technical limitation imposed by the lack of voltage clamp (see below). In fast twins, saturated photocurrent amplitude ranged from 26–92 pA (47.6 ± 21.74 pA; mean ± S.D., n = 21). The photocurrent reached to a peak in only 30–60 ms and it oscillated slightly during recovery of the dark current, and the decline of current from saturation after intense test flashes (10^7 photons/μm^2) was interrupted by a sustained plateau that persisted for up to several hundred milliseconds (Fig. 2). Again, in these cells with large capacitance (67.5 pF ± 21.69 mean ± S.D., n = 28), the kinetics of the photocurrent measured without voltage clamp are distorted.

The normalized peak amplitude-intensity relationship for common twin cones is illustrated in Fig. 3. These data were best fit by the Michaelis-Menten function, eqn. (2), and not by the exponential saturation function that best fits the data in single cones. From least-square fit of the function to experimental data, we estimate that in common twins σ was 1454 ± 730 photons/μm^2 (mean ± S.D., n = 51) and in fast twins σ was 9402 ± 4838 photons/μm^2 (mean ± S.D., n = 19) (Table 1).

Individual members of a twin pair exhibit identical photocurrents

Since the currents measured in twin cones with suction electrodes are the sum of the signals generated by each of the members of the cell pair, the features we measure might not be a reliable representation of the transduction signal from each individual cell. We found, however, that individual members of a twin pair

Table 1.

	Rods	Single cones	Common twin cones	Fast twin cones
Without voltage clamp:				
λ_{max} (nm)	528 ± 4.3 (7)	542 ± 3.2 (8)	605 ± 4.8 (10)	606 ± 6.5 (4)
i_{max} (pA)	36.7 ± 14.9 (11)	23.34 ± 8.21 (45)	33.98 ± 16.68 (57)	47.64 ± 21.74 (22)
i_{range} (min . . . max, in pA)	20.5 . . . 63	10.7 . . . 45	12.32 . . . 84.8	16 . . . 92
σ (photons·μm^{-2})	28.1 ± 7.07 (11)	238.0 ± 128.1 (42)	1454 ± 730 (51)	9402 ± 4838 (19)
I_{bo} (photons·$\mu m^{-2}\cdot s^{-1}$)	1.45 ± 0.66 (3)	1.81 × 10^3 ± 1.16 × 10^3 (11)	4.56 × 10^3 ± 2.17 × 10^3 (6)	6.79 × 10^4 ± 1.90 × 10^4 (6)
Kinetics:				
S_f^D (pA·photon$^{-1}\cdot\mu m^2$)	0.578 ± .369 (9)	0.1472 ± .0758 (12)	0.0808 ± 0.025 (23)	0.00753 ± 0.0040 (12)
time-to-peak (ms)	341.6 ± 63.8 (9)	165.7 ± 38.7 (12)	101.02 ± 18.51 (23)	57.13 ± 13.0 (12)
n (# stages)	3.13 ± 0.64 (9)	3.57 ± 0.18 (12)	6.4 ± 1.4 (23)	7.7 ± 0.67 (12)
Voltage clamped:				
i_{max} (pA)	n.d.	20.3 ± 7.48 (16)	26.93 ± 15.35 (23)	n.d.
i_{range} (min . . . max, in pA)	n.d.	10.5 . . . 42	7.3 . . . 70	n.d.
Capacitance (pF)	n.d.	56.53 ± 15.42 (28)	67.5 ± 21.69 (28)	n.d.
Capacitance range (pF)	n.d.	32 . . . 78	32 . . . 115	n.d.
Kinetics:				
A_1	n.d.	3.32 ± 1.2	6.132 ± 3.67	n.d.
$t_{peak,1}$	n.d.	0.086 ± 0.012	.0702 ± 0.0129	n.d.
n_1	n.d.	3.45 ± 0.69	4.83 ± 0.98	n.d.
A_2	n.d.	0.80 ± 0.40	1.123 ± 0.876	n.d.
$t_{peak,2}$	n.d.	0.19 ± 0.05	0.130 ± 0.026	n.d.
n_2	n.d.	7.25 ± 2.76	11.5 ± 2.07	n.d.
τ	n.d.	0.244 ± 0.08	0.142 ± 0.092	n.d.
Sample size	—	10	6	—

are essentially identical to each other in their response characteristics. To demonstrate this, we compared the photocurrents generated in an intact twin cone with those measured after one of the outer segments in the pair was destroyed with a fine glass needle. Fig. 4 illustrates photocurrents measured in a twin pair with its inner segments drawn into a suction electrode. By convention, the photocurrents are now negative in polarity. Fig. 4 compares the currents generated by an identical family of light flashes when both outer segments were intact and after destroying one of them. In this and two other identical experiments, the destruction of one outer segment reduced the amplitude of the photocurrent at each intensity by 50 ± 4.8% (mean ± S.D.) but hardly changed its time course. Detailed comparison of the photocurrents measured with both outer segments intact or with only one outer segment in place reveals that currents were reduced by half in amplitude but were otherwise nearly superimposable (Fig. 4). The loss of an outer segment caused a very slight increase in response kinetics, presumably because of a decrease in membrane capacitance since the cells were not voltage clamped. In three additional cells, we succeeded in removing only part of the outer segment. Partially removing an outer segment resulted in a reduction in photocurrent amplitudes that were less than 50%; however, the reduced photocurrents were still superimposable on those measured in the intact pair by applying scaling factors between 1 and 2. Thus, the signals we measured in twin cones were simply the sum of two identical signals, each coming from the individual members of the pair.

Action spectra

We constructed action spectra for rods, single cones, and twin cones by measuring their photocurrent peak amplitudes with suction electrodes. The details of our protocol are described in the Methods section. Spectra are shown in Fig. 5. On the basis of these analyses, we identified rod and cone visual pigments with the following spectral properties: rod, λ_{max} = 528 ± 4.3 nm (n = 7); single cone, λ_{max} = 542 ± 3.2 nm (n = 8); and twin cone, λ_{max} = 605 ± 4.8 nm (n = 10). Conventional twins (Fig. 5, filled circles) and fast twins (Fig. 5, open circles) contain visual pigments that exhibit indistinguishable spectral properties. The action spectra data were well fit by Dartnall nomograms of the appropriate λ_{max} designed to describe the absorption spectra of visual pigments containing A-2 retinal chromophore (Dawis, 1981).

In some teleost species, individual members of a twin pair contain different photopigments (Levine et al., 1979). In striped bass both members of the twin pair contain the same pigments since the spectral sensitivity data for twin pairs measured with both outer segments in the electrode were well fit by the Dartnall nomogram for a single visual pigment of λ_{max} = 605 nm. Moreover, we were able to determine the spectral sensitivity of twin cones before and after one of the outer segments was mechanically removed as described above. In each case, the spectral sensitivity of the photocurrents was the same before and after removing one of the outer segments and identical to that presented in Fig. 5.

Kinetics of the photocurrent

Rods

The time course of the rod photocurrent measured with suction electrodes was well described by the impulse response of a filter with n stages [eqn. (4)]. Best fits were obtained with the values of the adjustable parameters listed in Table 1. These values are essentially identical to those that best fit the response in rods of comparable dimensions in the retinae of rats (Penn & Hagins, 1972) or monkey (Baylor et al., 1984), when the values of t_{peak} are adjusted for temperature with a Q_{10} of 1.8 (Baylor et al., 1974).

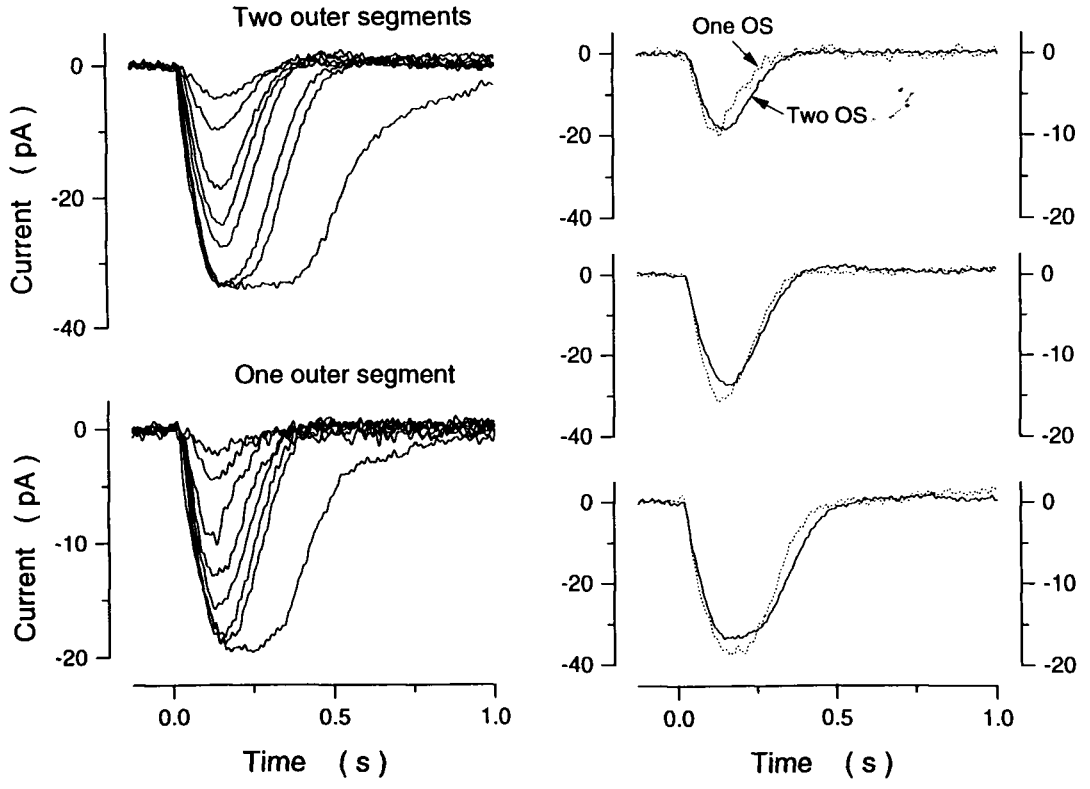

Fig. 4. Photocurrents measured in the same solitary twin cone either with both outer segments intact or after removing the outer segment from one of the members of the pair. Photocurrents were measured with a suction electrode engulfing both cone inner segments, by convention; therefore, photocurrents are illustrated as negative in polarity. Photocurrents were elicited in two successive trials by identical 10-ms duration flashes of 606-nm light that delivered 124, 248, 496, 992, 1984, 3969, 7789, and 7.788 × 10^4 photons/μm^2. Removal of one outer segment reduced the photocurrents amplitude almost exactly by half, without altering their waveform. The panels on the right compare in detail the photocurrents recorded either in the intact twin (continuous line) or after removing one of the outer segments (interrupted line) in response to identical flashes at three intensities (in photons/μm^2): 496 (upper panel), 992 (middle panel), or 7789 (lower panel).

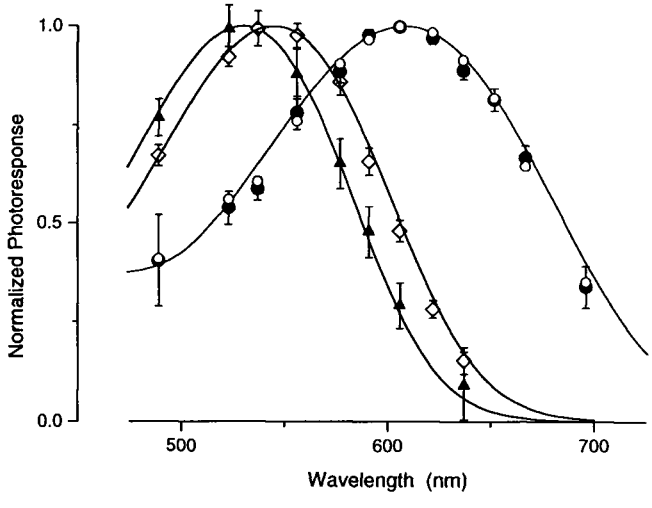

Fig. 5. Action spectra of the photocurrent of rods (▲), single cones (◇), common twin cones (●), and fast twin cones (○). The photosensitivity at each wavelength was normalized by the maximum photosensitivity. Points are the average (±S.D.) of data from 7 rod clusters, 8 single cones, 10 common twin, and 4 fast twins. The continuous line is an optimized fit to the data of a polynomial nomogram that describes the absorption spectrum of vitamin A2-based visual pigments (Dawis, 1981). The λ_{max} in the nomograms that best fit the data were: rods, 528 nm ±4.3; single cones, 542 nm ±3.2; common twins, 605 nm ±4.8; and fast twins, 606 nm ±6.5.

Single cones

A photocurrent with the linear range of response dynamics measured in a single cone with a suction electrode is illustrated in Fig. 6. Superimposed on the current tracing is an optimized fit to the data of eqn. (4). The adequacy of the impulse response to describe photocurrent kinetics of single cones at early times in the flash was generally better than at times greater than twice the time to peak. Table 1 lists that average value of the adjustable parameters needed to fit the kinetics of the dim light photocurrent in 12 different cells.

Although studies of photocurrent sensitivity and action spectra measured with suction electrodes alone are technically reliable, kinetic studies are potentially misleading because there is no control of membrane voltage. Lack of voltage clamp introduces potential kinetic distortions in the current measurements for two major reasons: first, the current that charges (and discharges) membrane capacitance as voltage changes is not separated from the ionic current and second, the possible voltage dependence of the membrane current yields time-dependent changes that may reflect changes in the membrane voltage and not in conductance. Kinetic distortions in the absence of voltage clamp are serious in bass cone photoreceptors both because membrane capacitance is large (singles: 56.53 pF ± 15.42, mean ± S.D., n = 28; twins 67.50 pF ± 21.69, mean ± S.D., n = 28) and because the photocurrent is voltage dependent over the range of the photovoltage (Miller & Korenbrot, 1992).

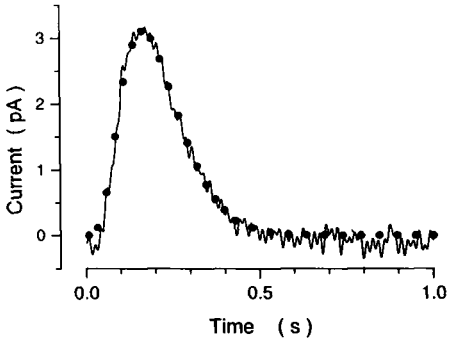

Fig. 6. Kinetics of dim light photocurrent in dark-adapted single cones in the absence of voltage clamp. Data is the signal average of eight successive trials measured with a suction electrode in response to a 10-ms flash of 540 nm that delivered 65 photons/μm^2. The response shown was within the linear range of the cone's response range since in this cell the intensity necessary to half-saturate the photoresponse was 254 photons/μm^2. Superimposed on the data, and illustrated as filled circles, is the optimized fit of a function that describes the impulse response of a sequence of n irreversible, first-order reactions [text eqn. (4)]. The values of adjustable parameters that yielded the fit as shown were A = 3.1 pA, t_{peak} = 167 ms, and n = 4.

To reliably measure the kinetics of the photocurrent in single cones, we measured the outer-segment current with a suction electrode, while we simultaneously clamped membrane voltage at −40 mV with a tight-seal electrode applied to the inner segment. In darkness, membrane current was near zero at −40 mV, which we therefore took to be near the resting membrane potential of these cells. Fig. 7 illustrates photocurrents measured in the same single cone either in the absence of voltage clamp or while holding the membrane potential at −40 mV. Photocurrents were generated by 10-ms flashes of 540-nm light of varying intensities. Essentially the same results were obtained in all 23 cells studied with this protocol. Under voltage clamp, but not in its absence, the initial rate of rise of the photocurrent increased in proportion to flash intensity, without reaching a limiting value over the intensity tested. Also the time to peak progressively decreased as light intensity increased. The most apparent change occurred in the recovery portion of the photocurrent: under voltage clamp, the time course of recovery was accelerated and an undershoot appeared at the end of the response (Fig. 7).

The kinetics of the linear-response photocurrents of voltage-clamped single cones were well described by the modified impulse-response function presented as eqn. (5). Fig. 8 illustrates a linear-response photocurrent measured under voltage clamp in a single cone. Superimposed on the current tracing is an optimized fit of eqn. (5) to the data. The average values of the adjustable parameters that best fit data measured in ten different cells are summarized in Table 1.

Twin cones

Linear-range photocurrents measured in common and fast twins in the absence of voltage clamp are shown in Fig. 9. These data were well fit by the impulse-response function, eqn. (4). The average values of adjustable parameters that yielded optimum fits are listed in Table 1. We also studied photocurrents of twin cones under voltage clamp to obtain reliable measurements of their time course. Fig. 10 illustrates photocurrents measured in the same common twin cone either in the absence of

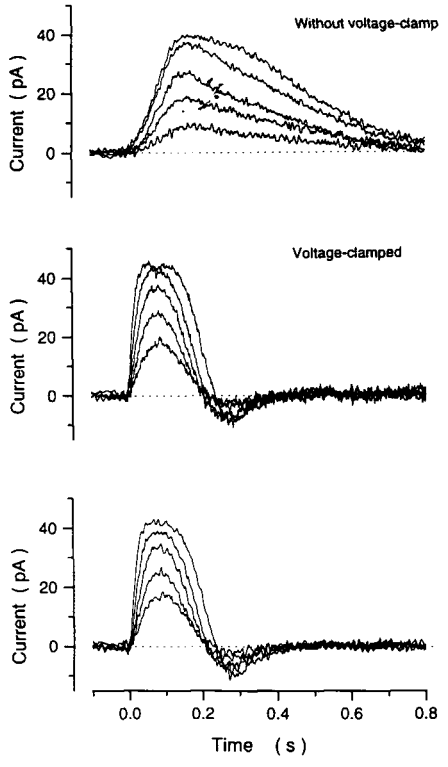

Fig. 7. Photocurrents measured in the same single cone with and without voltage clamp. The upper panel shows photocurrents measured first with a suction electrode alone and thus, in the absence of voltage clamp. The cone was then whole-cell voltage-clamped with a tight-seal electrode. The middle panel illustrates the photocurrents measured with the tight-seal electrode at a holding voltage of −40 mV, while the lower panel illustrates the currents measured simultaneously with the suction electrode. The holding current at −40 mV was −10 pA. Photocurrents in both sets of data were elicited by 10-ms flashes of 540-nm light of intensities equal to 145, 297, 582, 1379, and 2746 photons/μm^2.

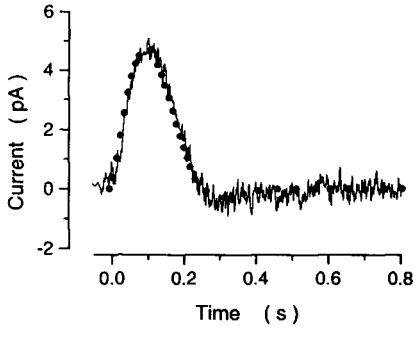

Fig. 8. Kinetics of dim light photocurrent in a voltage-clamped, dark-adapted single cone. Photocurrent was measured with a tight-seal electrode at −40 mV holding voltage in response to a 10-ms flash of 540 nm that delivered 58 photons/μm^2. The response shown was within the linear range of the cone's photosensitivity since in this cell the intensity necessary to half-saturate the photoresponse was 103 photons/μm^2. Superimposed on the data, and illustrated as filled circles, is the optimized fit of an empirical function presented as text eqn. (5). The values of adjustable parameters that yielded the fit as shown were A_1 = 4.76 A, t_{peak1} = 108 ms, $n1$ = 3, A_2 = 0.987 A, t_{peak2} = 215 ms, $n2$ = 11, and τ = 243 ms.

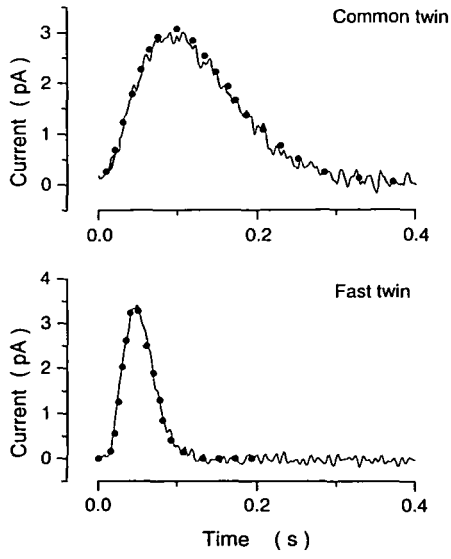

Fig. 9. Kinetics of dim light photocurrent in dark-adapted common and fast-type twin cones measured with suction electrodes without voltage clamp. Data for the common twin is the signal average of four responses, while for the fast twin it is the average of eight trials. For the common twin the response was elicited by 10-ms flashes of 606 nm that delivered 51.4 photons/μm^2. The response shown was within the linear range of the cone's photosensitivity since in this cell the intensity necessary to half-saturate the photoresponse was 523 photons/μm^2. Superimposed on the data, and illustrated as filled circles, is the optimized fit of a function that describes the impulse response of an irreversible sequence of first-order reactions [text eqn. (4)]. The values of adjustable parameters that yielded the fit as shown were $A = 3.07$ A, $t_{peak} = 105$ ms, and $n = 4$. For the fast twin the response was elicited by 10-ms flashes of 606 nm that delivered 952 photons/μm^2. This was a linear-range response since half-saturation intensity for the cell was 6264 photons/μm^2. The filled circles illustrate the best fit of text eqn. (4) to the data. The values of adjustable parameters that yielded the fit as shown were $A = 3.4$ A, $t_{peak} = 46$ ms, and $n = 8$.

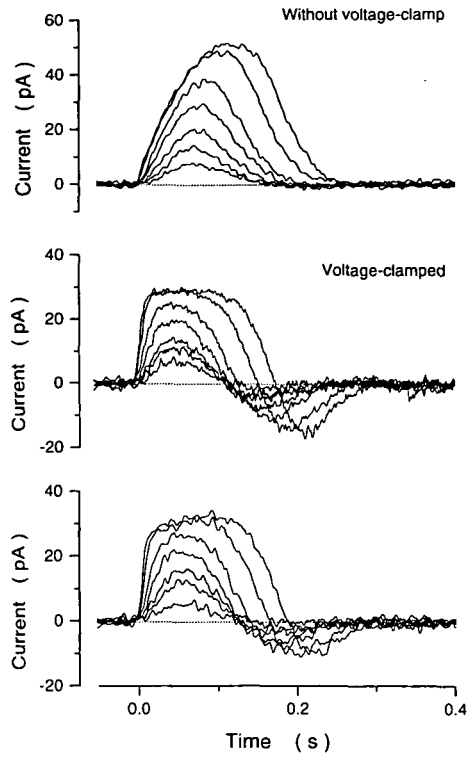

Fig. 10. Photocurrents measured in the same common twin cone with and without voltage clamp. The upper panel shows photocurrents measured first in the absence of voltage clamp with a suction electrode alone engulfing the outer segment of both members of the pair. The cone was then whole-cell voltage-clamped with a tight-seal electrode applied to the inner segment of one member. The middle panel illustrates the photocurrents measured with the tight-seal electrode at a holding voltage of −40 mV, while the lower panel illustrates the currents measured simultaneously with the suction electrode. The photocurrent measured under voltage clamp was the same in the suction and tight-seal electrodes. Photocurrents in both sets of data were elicited by 10-ms flashes of 620-nm light of intensities equal to 310, 615, 1288, 2593, 5138, 1.47×10^4, and 3.032×10^4 photons/μm^2.

voltage clamp or under voltage clamp while holding the membrane potential at −40 mV. Photocurrents were generated by 10-ms flashes of 610-nm light of varying intensities. The same results were obtained in all ten cells studied with this protocol. Similar to the findings in single cones, the initial rate of rise of the photocurrent under voltage clamp was faster than in its absence and the response reached to a peak earlier in time. The rate of rise increased with light intensity and did not saturate over the intensities tested. The recovery of the photocurrent at the end of the response was also faster and an undershoot was apparent. These data are a more faithful representation of the kinetic characteristics of transduction in the cones than are measurements with suction electrodes alone.

We were surprised to find that the amplitude of the photocurrents measured in the suction electrode and the tight-seal electrode were very similar since the suction electrode measured the current from both members of the pair, but the tight electrode was applied to only one of the cells. This observation suggested that the members of a twin pair are electrically coupled.

To investigate whether members of a twin pair are electrically coupled, we explored the effects of membrane voltage on the photocurrent. The photocurrent in bass cones reverses in direction between +10 and +15 mV (Miller & Korenbrot, 1992). If the members of a twin pair are electrically coupled, then the voltage control obtained in the cell attached to the tight-seal electrode should also be observed in the second cell. If this is the case, then photocurrents measured with the suction electrode when the membrane voltage is near the reversal potential should be very small in amplitude. On the other hand, if members of the twin pair are not electrically coupled, when membrane voltage in one cell is held near the reversal potential, the suction electrode should still record a normal, but smaller amplitude photocurrent generated by the non-voltage clamped member of the pair. The results from one such experiment are presented in Fig. 11. Three suction electrode records are displayed. A control sweep at −40 mV exhibits a normal, voltage-clamped photocurrent of 21 pA amplitude. During the second sweep, the voltage was stepped to +20 mV prior to the test flash. The test flash generated a very small photocurrent, less than 2 pA in amplitude, of inverted polarity. Finally, a third sweep was recorded after returning to −40 mV showing the complete recovery of photocurrent kinetics and amplitude. Identical results were obtained in three cells tested with this protocol. Since the photocurrent measured with the suction electrode essentially vanished near the reversal potential, then the voltage in both members of the pair must have been near the reversal potential for the

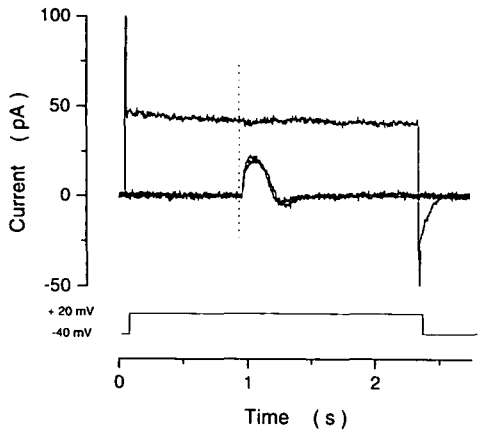

Fig. 11. The members of a common twin cone are electrically coupled. Shown are currents measured with a suction electrode that engulfed both outer segments of a twin pair, while membrane voltage was clamped through a tight-seal electrode attached to the inner segment of one of the cells in the pair. Photocurrents were elicited by 10-ms flashes of bright 620-nm light that delivered 1.47×10^4 photons/μm^2. Flashes were presented at the moment indicated by the dashed vertical line. To test the effects of voltage on the photocurrent kinetics, flashes were presented at the holding voltage (−40 mV) or after stepping the voltage to +20 mV. Superimposed at −40 mV are photocurrents measured before and after having stepped to +20 mV. The reversal potential of the photocurrent in these cells was about +16 mV. At +20 mV, the photocurrent in both members of the twin pair, as measured with the suction electrode, was of a very small negative amplitude even though the tight-seal electrode was attached to only one of the members. This result indicates that the members of the twin pair are electrically coupled since voltage control applied to only one cell also clamps the membrane potential of its twin.

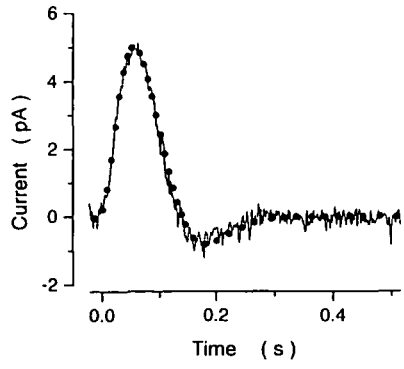

Fig. 12. Kinetics of dim light photocurrent in a voltage-clamped, dark-adapted common twin cone. Photocurrent was measured with a suction electrode while holding membrane voltage at −40 mV with the simultaneous use of a tight-seal electrode. The response was elicited by 10-ms flash of 620 nm that delivered 240.4 photons/μm^2. This was a linear-range response since half-saturation intensity for the cell was 1369 photons/μm^2. Superimposed on the data, and illustrated as open triangles, is the optimized fit of an empirical function presented as text eqn. (5). The values of adjustable parameters that yielded the fit as shown were $A_1 = 5.05$ A, $t_{peak1} = 64.3$ ms, $n1 = 4$, $A_2 = 1.02$ A, $t_{peak2} = 143$ ms, $n2 = 12$, and $\tau = 179$ ms.

photocurrent. This could only be achieved if the cells were electrically coupled.

Since the members of a twin pair contain the same visual pigment, transduce with identical characteristics and are electrically coupled, then the photocurrents measured under voltage clamp reliably measure the transduction signals from each member cell. The kinetics of the linear-response photocurrents of voltage-clamped twin cones were well described by the modified impulse-response function, eqn. (5). Fig. 12 presents a representative photocurrent of a common twin cone measured under voltage clamp along with optimized fits to the data of eqn. (5). The average results of fits to ten individual common twin cones are summarized in Table 1. Despite repeated efforts over a 9-month period, we were unable to find fast twins during voltage-clamp experiments.

Light adaptation

Single cones

Background light reduces the peak amplitude of the photocurrent and accelerates its time course. The responses of a single cone to a flash of constant intensity presented in the dark or superimposed on a step of background light of varying intensities are presented in Fig. 13. Photocurrents were measured with suction electrodes alone. The initial amplitude of the response to the background step increased with the intensity of this step. These responses decayed from an initial value to a steady state at a rate that changed with light intensity. Test flashes in the linear range of the photoresponse were delivered after the photocurrent had reached steady state. In Fig. 13, the displayed photocurrents are offset to make the steady-state amplitude the same at all background intensities.

The photocurrent generated by the test flash decreased in peak amplitude as a function of the intensity of the background light. This dependence for all single cones studied is illustrated in Fig. 13. Peak photocurrent amplitude was normalized by dividing the amplitude at each background light by the amplitude measured in the dark-adapted state. Adapting light intensities were normalized by dividing the intensity by that required to reduce the amplitude of the linear-response photocurrent by 50%. The experimental results were well described by the Weber-Fechner function [eqn. (6)] (Fig. 13). For 11 single cones, the average I_{bo} was $1.81 \times 10^3 \pm 1.16 \times 10^3$ photons/$\mu m^2 \cdot s$ (mean ± S.D., range $0.628\text{–}3.99 \times 10^3$ photons/$\mu m^2 \cdot s$) (Table 1).

The acceleration of photocurrent kinetics in light-adapted single cones is illustrated in Fig. 14. Dark-adapted and light-adapted photocurrents have been normalized with respect to photocurrent amplitude. The t_{peak}'s of photocurrents following the onset of the light step and test flashes were reduced as the intensity of the test flash was increased. The reduction of t_{peak} was more subtle than changes in photocurrent amplitude and waveform. t_{peak} was reduced from 172 ± 34 ms in dark-adapted cells to 106 ± 12 ms in the presence of adapting light near I_{bo} (values are mean ± S.D., $n = 9$).

Common and fast twin cones

Adapting backgrounds changed the amplitude and time course of the flash response in common and fast twins with qualitatively similar characteristics as those observed in single cones. Fig. 15 illustrates the responses of both a common and a fast twin to constant test flashes in the linear range, delivered in dark-

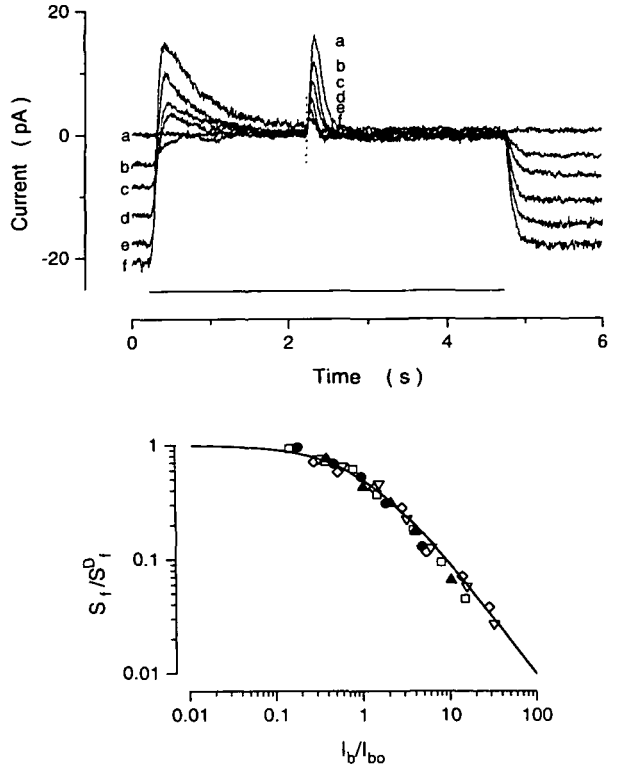

Fig. 13. Light adaptation in a single cone. The upper panel illustrates outer segment currents were measured with suction electrodes. At the time, and for the duration indicated by the horizontal bar above the time axis, a background light of 540 nm of varying intensity was presented to the photoreceptor. Test photocurrents superimposed on the background light were elicited by 10-ms flashes of 540-nm light that delivered a constant 129 photons/μm^2 at the time indicated by the dashed vertical line. The intensity of the test flash was within the linear range of response of the cone (σ = 296 photons/μm^2). To compare the effects of background light on the test response, we draw the current traces so that they superimpose at the steady-state amplitude obtained with the background light on. With this convention, the current in darkness has a value of 0 pA in the dark-adapted cone and it takes progressively more negative values as the background intensity increases in amplitude. The relaxation in current amplitude from a peak value immediately after the onset of background illumination to a steady-state value is itself evidence of light adaptation in the cones. The extent of this relaxation increased as the intensity of the background rose. The response to the constant intensity flash was largest in amplitude in the dark-adapted cone and became progressively smaller as the intensity of the background increased. Background intensities tested were (in photons/$\mu m^2 \cdot s$): (a) 0 (dark-adapted); (b) 310; (c) 580; (d) 1500; (e) 3100; and (f) 5800. The lower panel illustrates the normalized photosensitivity of five different cones, each identified by a different symbol, measured in the steady state as a function of the intensity of an adapting background light. The intensity of the background light was normalized by dividing each intensity tested, I_b, by I_{bo}, the background intensity necessary to reduce the photosensitivity by half. The continuous line is an optimized fit to the data of the Weber-Fechner law [text eqn. (6)]. The average value of I_{bo} was 1.81 × 10^3 photons/$\mu m^2 \cdot s$ (Table 1).

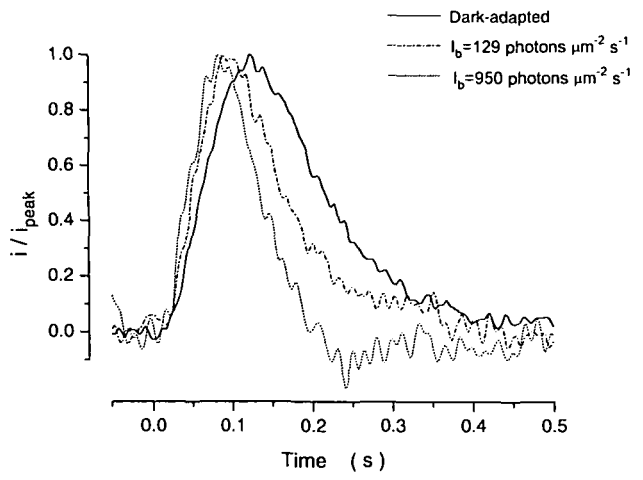

Fig. 14. Background light accelerates the time to peak of the photocurrent in single cones. Photocurrents measured with a suction electrode alone were elicited by a 10-ms flash of 540 nm that delivered 129 photons/μm^2. The flash was presented to a dark-adapted cell (continuous line) or against a steady background of 540-nm light at either of two intensities (in photons/$\mu m^2 \cdot s$): 580 (dash-dot-dash) or 3100 (dashed line). To compare their time course, the photocurrents were normalized to the same peak amplitude.

ness or in the presence of adapting light. In both cell types, the flash photocurrent becomes smaller in amplitude and faster in time course as the intensity of the adapting background increases.

Fig. 15 illustrates the dependence of the flash sensitivity of twin cones on the intensity of the background light. To compare data among different cells, flash sensitivity and background intensity were normalized as described above. Experimental data for both common and fast twins were well fit by the Weber-Fechner function [eqn. (6)]. For common twins, I_{bo} average was 4.56 × 10^3 ± 2.17 × 10^3 photons/$\mu m^2 \cdot s$ (mean ± S.D., range from 1.35 × 10^3–7.41 × 10^3 photons/$\mu m^2 \cdot s$, n = 6). For fast twins, I_{bo} average was 6.79 × 10^4 ± 1.90 × 10^4 photons/$\mu m^2 \cdot s$ (± S.D., range from 5.35 × 10^4–9.22 × 10^4 photons/$\mu m^2 \cdot s$, n = 6) (Table 1).

The kinetics of common twin-cone transduction signals were accelerated in the presence of adapting light. In 14 different common twin cones, the time to peak was reduced from 114 ± 17 ms in dark-adapted cells to 69.5 ± 10 ms in the presence of adapting light near I_{bo}. Fast twins exhibited only a modest reduction in time to peak, from 64 ± 11 ms in dark-adapted cells to 61 ± 13 ms in the presence of adapting light near I_{bo} (n = 8). The change in waveform accompanying light adaptation in twins was dominated by reduction in response amplitude and only modest acceleration in kinetics. Because these measurements were conducted with suction electrodes alone, without voltage clamp, the modest effects on kinetics are likely to be distorted because of technical limitation in the recording technique as discussed above. Nonetheless, we present the data so it may be compared with adapted signals in other cone photoreceptors, most commonly also measured in the absence of voltage clamp.

Discussion

Dissociation of striped bass retina yields rods, green-sensitive single cones, and electrically coupled, red-sensitive twin cones. The isolated cones lack the nuclear region of the inner segment and the synaptic pedicle, yet they respond to light with characteristics indistinguishable from those measured in the intact ret-

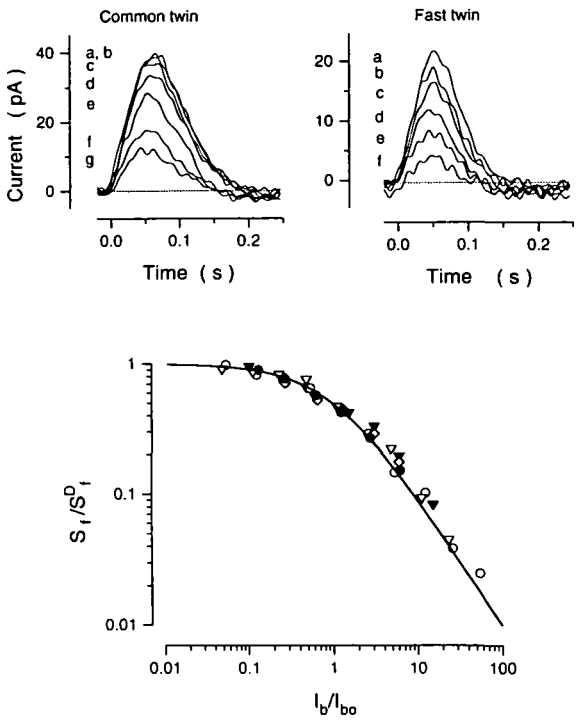

Fig. 15. Light adaptation in common and fast twins. The upper left panel displays photocurrents measured in a common twin cone in response to a constant 10-ms flash of 620 nm of 952 photons/μm^2 intensity delivered at time 0, and superimposed in the steady state on a continuous background of 620-nm light of intensities (in photons/μ^2·s): (a) dark-adapted; (b) 1.3×10^3; (c) 2.6×10^3; (d) 6.1×10^3; (e) 1.25×10^4; (f) 2.6×10^4; and (g) 6.1×10^4. The upper right panel displays photocurrents measured in a fast twin cone in response to a constant 10-ms flash of 620 nm of 4759 photons/μm^2 intensity delivered at time 0, and superimposed in the steady state on a continuous background of 620-nm light of intensities (in photons/μm^2·s): (a) dark-adapted; (b) 6.1×10^3; (c) 1.25×10^4; (d) 2.6×10^4; (e) 6.1×10^4; and (f) 1.25×10^5. The lower panel illustrates the normalized photosensitivity of three different common twin cones (filled symbols) and two fast twin cones (open symbols) measured in the steady state as a function of the intensity of an adapting background of 620-nm light. The intensity of the background light was normalized by dividing each intensity tested, I_b, by I_{bo}, the background intensity necessary to reduce the photosensitivity by half. The continuous line is an optimized fit to the data of the Weber-Fechner law [text eqn. (6)]. Although the dependence of photosensitivity on background intensity is of the same form in both types of twin cones, the intensity necessary to change photosensitivity by half, the value of I_{bo}, is very different. For common twins average I_{bo} was 4.56×10^3 photons/μm^2·s, while for fast twins it was 6.79×10^4 photons/μm^2·s (Table 1).

ina. Marchiafava et al. (1985) first reported the successful isolation of functional cone photoreceptors from the retina of tench. In the tench, too, the isolated photoreceptors are structurally incomplete. Incomplete cones from teleost are particularly useful in studies of phototransduction because they are large, abundant, and sturdy. However, they are of limited value in studies of signal processing since the missing regions of the inner segment contain ion channels important in shaping the photoresponse waveform and in synaptic function. Thus, in the solitary cones of bass we could not find voltage-sensitive Ca^{2+} channels, Ca^{2+}-dependent Cl-channels, or Ca^{2+}-dependent K^+ channels found in intact cones isolated from lizard or tiger salamander retinas (Maricq & Korenbrot, 1988; Barnes & Hille, 1989; Maricq & Korenbrot, 1990).

Cone photoreceptors in bass are less sensitive to light, respond with faster kinetics, and adapt over a wider range of light intensities than do rods (Table 1). The flash sensitivity of the rod photoresponse in striped bass is very similar to that of comparably sized rods in higher vertebrates such as rat (Hagins et al., 1970) or monkey (Baylor et al., 1984). Cone photoreceptors, in contrast, are much less stereotyped in their photoresponse. A range in flash sensitivities and kinetics of cone responses can be found when comparing anatomical subtypes both within the same retina and across species. Thus, in the retina of bass the response kinetics, photosensitivity and adaptation features differ significantly among single cones, common twin cones, and fast twin cones (Fig. 2, Table 1). Perry and McNaughton (1991) have described three types of single-cone photoreceptors in the tiger salamander retina which exhibit flash sensitivities differing by 15-fold. Surprisingly, Burkhardt et al. (1986) did not find differences in the sensitivities of single and twin cones in the walleye.

It is interesting to note that the values of the flash sensitivity of the cone photoresponse reported in the literature are not a continuum but fall into discrete values. Thus, single cones in striped bass and in walleye (Burkhardt et al., 1986) and red-sensitive single cones in tiger salamander (Schnapf & McBurney, 1980; Hestrin & Korenbrot, 1990; Perry & McNaughton, 1991) have similar flash sensitivities. The common twin cones in bass are about sixfold less sensitive and are very similar in sensitivity to all three types of single cones (red, blue, and green sensitive) in macaque monkey (Schnapf et al., 1990). Least sensitive are the fast twins in bass, which exhibit flash sensitivities and response kinetics comparable to those of the single cones of the ground squirrel (Kraft, 1988). Cones that share comparable values of flash sensitivity are not generally similar in other features, such as size or spectral sensitivity. If we assume that the molecules of transduction are the same in all cones, the discreteness in flash-sensitivity values suggests that there exist only a small number of molecular designs that control the ensemble behavior these molecules may take.

The use of extracellular measurements of membrane current has been extremely successful in studies of phototransduction in rods because, fortuitously, in these cells membrane capacitance is small (typically less than 15 pF) and the light-sensitive current is voltage independent over the range of changes caused by light (Baylor & Nunn, 1986). In cones, in contrast, membrane capacitance is large and the photocurrent is voltage dependent at all physiological values (Attwell et al., 1982; Perry & McNaughton, 1991; Miller & Korenbrot, 1992) limiting the value of studies of extracellular membrane currents alone. Voltage-clamped photocurrents were first measured in tiger salamander single cones by Attwell et al. (1982) with intracellular electrodes, and Perry and McNaughton (1991) have recently carried out a complete study in the same species with the simultaneous use of suction and tight-seal electrodes. In our studies in teleost cones, as in those of Perry and McNaughton (1991), photocurrents measured as extracellular currents differed in kinetics in the presence and absence of voltage clamp, but not in peak amplitude or light sensitivity. Kinetic data measured under voltage clamp reflects directly the time course of the transduction process. In both single and twin bass cones under voltage clamp, the response to flashes of light exhibits an un-

dershoot in its recovery phase that is not observed in the absence of voltage clamp. In the small cones of the monkey, similar oscillations at the end of flash photocurrents are measured with suction electrodes in the absence of voltage clamp (Schnapf et al., 1990). The small size of these cells suggests that their capacitance is small and, therefore, kinetic distortion in currents measured in the absence of voltage clamp are likely to be modest.

In our experiments, given the membrane capacitance of the isolated cone photoreceptors (on average 56 pF for singles and 67 pF for twins), the acceleration in photocurrent kinetics under voltage clamp was greater than expected if kinetics were only limited by capacitative elements in the simplest possible RC electrical circuit. The change in kinetics we observed could suggest that whole-cell recording perturbed transduction, perhaps by internal dialysis of an unidentified component. We do not believe this to be the case, because we found that the change in photocurrent kinetics was apparent as quickly as we were able to record photocurrents after obtaining whole-cell recordings (*ca.* 7 s) and remained stable for the duration of the experiment. For the composition of the cytoplasmic space to change upon whole-cell clamping, it would be required that small molecules in the cell come to equilibrium in their concentration with the pipette filling solution within 7 s. This is physically impossible given the known diffusion rates of small molecules in rod photoreceptors (Hochstrate & Ruppel, 1980). The changes in kinetics upon voltage clamp in the large teleost cones we have studied are likely to reflect complexities of the equivalent electrical circuit that best represents these cells.

The low prevalence of fast twins and their indistinguishable morphology from "common twins" raise the possibility that they might, in fact, be light-adapted common twins. This is not the case because: (1) We consistently failed in our attempts to convert common twins into fast twins by simply measuring responses against various intensities of background light. (2) The peak photocurrent amplitude of fast twins was consistently larger than those of common twin cones, in contrast to the fact that light-adapted cells have smaller photocurrent peak amplitudes than dark-adapted ones. (3) The characteristics of light adaptation in fast twins are distinct from those of common twins. The mean value of I_{bo} for fast twins is more than tenfold higher than for common twins.

Fast twins are rarely found in animals younger than 11 months (*ca.* 15 cm in length). Among the 118 twin-cone photocurrents recorded from animals younger than 10 months of age ($\leq$*ca.* 15 cm), only three fast twins were encountered (2.5%), whereas among the remaining 54 twin-cone photocurrents recorded from animals older than 10 months (>*ca.* 20 cm), 18 were fast twins. We suggest that "fast" twins are a subclass of receptors that appear late in the development of the bass retina. Previous experiments have documented changes in the population of cone photoreceptors as development progresses. Boehlert (1978) showed that in rockfish (*Sebastes diploproa*) single cones are lost and are replaced by twin cones in response to developmental clues as well as changes in the environment. Burkhardt et al. (1980) report that the retina of the juvenile walleye contains only single cones while the mature retina contains twice as many twin cones as single cones. In trout, UV sensitive cones disappear as the animals mature (Bowmaker & Kunz, 1987). It is presently unknown whether the changes in cone photoreceptor population arise from the delayed differentiation of new cells or from transformation of previously existing ones. Future work in striped bass may help answer this query as well as provide a system for the systematic exploration of the molecular mechanisms that may explain the differences in the function of rods and cones; differences that exist although the principal enzymes of phototransduction are not profoundly different in the two receptor types (Hestrin & Korenbrot, 1990).

References

Ali, M.A. & Anctil, M. (1976). *Retinas of Fishes: An Atlas.* Berlin-New York: Springer Verlag.

Attwell, D., Werblin, F.S. & Wilson, M. (1982). The properties of single cones isolated from the tiger salamander retina. *Journal of Physiology* **328**, 259–283.

Barnes, S. & Hille, B. (1989). Ionic channels of the inner segment of tiger salamander cone photoreceptors. *Journal of General Physiology* **94**, 719–744.

Baylor, D.A. (1987). Photoreceptor signals and vision. *Investigative Ophthalmology and Visual Science* **28**, 34–49.

Baylor, D.A. & Fuortes, M.G.F. (1970). Electrical responses of single cones in the retina of the turtle. *Journal of Physiology* **207**, 77–92.

Baylor, D.A., Hodgkin, A.L. & Lamb, T.D. (1974). The electrical response of turtle cones to flashes and steps of light. *Journal of Physiology* **242**, 685–727.

Baylor, D.A., Lamb, T.D. & Yau, K.-W. (1979). The membrane current of single rod outer segments. *Journal of Physiology* **288**, 589–611.

Baylor, D.A. & Nunn, B.J. (1986). Electrical properties of the light-sensitive conductance of rods of the salamander *Ambystoma tigrinum*. *Journal of Physiology* **371**, 115–145.

Baylor, D.A., Nunn, B.J. & Schnapf, J.L. (1984). The photocurrent, noise and spectral sensitivity of rods of the monkey, *Macaca fascicularis*. *Journal of Physiology* **357**, 575–607.

Boehlert, G.W. (1978). Intraspecific evidence for the function of single and double cones in the teleost retina. *Science* **202**, 309–311.

Bowmaker, J.K. & Kunz, Y.W. (1987). Ultraviolet receptors, tetrachromatic color vision and retinal mosaics in the brown trout (*Salmo trutta*): Age-dependent changes. *Vision Research* **27**, 2101–2108.

Burkhardt, D.A., Hassin, G., Levine, J.S. & MacNichol, E.F., Jr. (1980). Electrical responses and photopigments of twin cones in the retina of the walleye. *Journal of Physiology* **309**, 215–228.

Burkhardt, D.A., Kraft, T.W. & Gottesman, J. (1986). Functional properties of twin and single cones. *Neuroscience Research* **4**, S45–S58.

Cherr, G.N. & Cross, N.L. (1987). Immobilization of mammalian eggs on solid substrates by lectins for electron microscopy. *Journal of Microscopy* **145**, 341–345.

Cohen, A.I. (1972). *Rods and Cones. Handbook of Sensory Physiology, Vol. 7*, Berlin-New York: Springer-Verlag.

Dawis, S.M. (1981). Polynomial expressions of pigment nomograms. *Vision Research* **21**, 1427–1430.

Hagins, W.A., Penn, R.D. & Yoshikami, S. (1970). Dark current and photocurrent in retinal rods. *Biophysical Journal* **10**, 380–412.

Hamill, O.P., Marty, A., Neher, E., Sakmann, B. & Sigworth, F.J. (1981). Improved patch-clamp techniques for high-resolution current recording from cells and cell-free membrane patches. *Pfluger Archives* **391**, 85–100.

Hestrin, S. & Korenbrot, J.I. (1990). Activation kinetics of retinal cones and rods: Response to intense flashes of light. *Journal of Neuroscience* **10**, 1967–1973.

Hochstrate, P. & Ruppel, H. (1980). On the evaluation of photoreceptor properties by microfluorometric measurements of fluorochrome diffusion. *Biophysics of Structure and Mechanism* **6**, 125.

Kaneko, A. & Tachibana, M. (1985). Electrophysiological measurements of the spectral sensitivity of three types of cones in the carp retina. *Japanese Journal of Physiology* **35**, 355–365.

Kraft, T.W. (1988). Photocurrents of cone photoreceptors of the golden-mantled ground squirrel. *Journal of Physiology* **404**, 199–213.

Lamb, T.D., McNaughton, P.A. & Yau, K.W. (1981). Spatial spread of activation and background desensitization in toad rod outer segments. *Journal of Physiology* **319**, 463–486.

LEVINE, J.S., MACNICHOL, E.F., JR., KRAFT, T.W. & COLLINS, B.A. (1979). Intraretinal distribution of cone pigments in certain teleost. *Science* **204**, 523–526.

LOEW, E.R. & LYTHGOE, J.N. (1978). The ecology of cone pigments in teleost fish. *Vision Research* **18**, 715–722.

LYALL, A.H. (1957). The growth of the trout retina. *Quarterly Journal Microscopical Science* **98**, 101–110.

MARCHIAFAVA, P.L., STRETTOI, E. & ALPIGIANI, V. (1985). Intracellular recording from single and double cone cells isolated from the fish retina (*Tinca tinca*). *Experimental Biology* **44**, 173–180.

MARICQ, A.V. & KORENBROT, J.I. (1988). Calcium and calcium-dependent chloride currents generate action potentials in solitary cone photoreceptors. *Neuron* **1**, 503–515.

MARICQ, A.V. & KORENBROT, J.I. (1990). Potassium currents in the inner segment of single retinal cone photoreceptors. *Journal of Neurophysiology* **64**, 1929–1940.

MCNAUGHTON, P.A. (1990). Light response of vertebrate photoreceptors. *Physiological Reviews* **70**, 847–883.

MILLER, D.L. & KORENBROT, J.I. (1987). Kinetics of light-dependent Ca fluxes across the plasma membrane of rod outer segments: A dynamic model of the regulation of cytoplasmic Ca concentration. *Journal of General Physiology* **90**, 397–426.

MILLER, J.L. & KORENBROT, J.I. (1992). In intact retinal cones membrane depolarization activates the cGMP-dependent current in the dark: Evidence for Ca control of guanylate cyclase and phosphodiesterase. *Journal of General Physiology* (in press).

PENN, R.D. & HAGINS, W.A. (1972). Kinetics of the photocurrent of retinal rods. *Biophysical Journal* **12**, 1073–1094.

PERRY, R.J. & MCNAUGHTON, P.A. (1991). Response properties of cones from the retina of the tiger salamander. *Journal of Physiology* **433**, 561–587.

PICONES, A. & KORENBROT, J.I. (1992). Permeation and interaction of monovalent cations with the cGMP-gated channel of cone photoreceptors. *Journal of General Physiology* **100**, 647–673.

PUGH, E.N., JR. & COBBS, W.H. (1986). Visual transduction in vertebrate rods and cones: A tale of two transmitters, calcium and cyclic GMP. *Vision Research* **26**, 1613–1643.

PUGH, E.N., JR. & LAMB, T.D. (1990). Cyclic GMP and calcium: The internal messengers of excitation and adaptation in vertebrate photoreceptors. *Vision Research* **30**, 1923–1948.

RODIECK, R.W. (1973). *The Vertebrate Retina.* San Francisco, California: W.H. Freeman.

SCHNAPF, J.L. & MCBURNEY, R.N. (1980). Light-induced changes in membrane current in cone outer segments of tiger salamander and turtle. *Nature* **287**, 239–241.

SCHNAPF, J.L., NUNN, B.J., MEISTER, M. & BAYLOR, D.A. (1990). Visual transduction in cones of the monkey *Macaca fascicularis*. *Journal of Physiology* **427**, 681–713.

TOMITA, T. (1970). Electrical activity of vertebrate photoreceptors. *Quarterly Review of Biophysics* **3**, 179.

WALLS, G.L. (1942). *The Vertebrate Eye and Its Adaptive Radiation.* Bloomfield Hills, Michigan: Cranbrook Institute of Science.